Positron thermalization in Si and GaAs

J. Nissilä, K. Saarinen, and P. Hautojärvi

Laboratory of Physics, Helsinki University of Technology, P. O. Box 1100, FIN-02015 HUT, Finland
(Received 6 July 2000; published 3 April 2001)

Positron thermalization in Si and GaAs has been studied both by experiments and simulations. The decrease in the positron mean energy due to the interactions with longitudinal-acoustic phonons was calculated down to 4 K by solving numerically the Boltzmann equation for the positron momentum distribution. We find that the differences in the strength of the positron-phonon coupling can result in considerable variations in the thermalization time. At 10 K, the time needed by the positrons to reach twice the thermal energy is 25 ps in Si, and 80 ps in GaAs. We find experimental support for the calculated thermalization behavior by studying the temperature dependence of the positron trapping rate at negative vacancy-type defects in Si and GaAs. In Si, we observe that positron lifetime data depends strongly on the sample temperature at least down to 8 K, which supports the predicted fast thermalization. In GaAs, the trapping rate below 20 K is observed to increase considerably less than expected for positrons thermalized instantly after implantation. This demonstrates experimentally that the thermalization time in GaAs is indeed much longer than in Si. We show further that the calculated positron energy-loss rates can explain quantitatively the temperature dependence of the experimental trapping rate in GaAs down to 8 K.

I. INTRODUCTION

Positron thermalization in solids at low temperatures is an interesting and challenging problem that has been studied both experimentally and theoretically every now and then over the last 40 years. [1–7] Besides from the point of view of positron-host interactions, the problem is important also when considering positron annihilation studies of defects in solids. In analyzing the annihilation radiation data, it is generally assumed that the positron is in thermal equilibrium (or very near) with the host very soon after implantation (within 10 ps) even at 10 K. This assumption is widely accepted to be true irrespective of the material. The experimental support for these ideas is based on ACAR (angular correlation of annihilation radiation) measurements of positron momentum distribution at the time of annihilation in simple metals.[5] The experimental distribution seems to follow the Maxwell-Boltzmann (MB) distribution even down to liquid helium temperature within the experimental accuracy. A most impressive piece of data is related to positronium atoms in quartz at 4.2 K: even this neutral particle was found to thermalize to a temperature of 10 K within the average lifetime of 125 ps.[4] This points out that phonon scattering is efficient in reducing the positron or positronium energy.

The rapidity of positron thermalization is supported by the theoretical calculations in aluminum by Jensen and Walker.[7] They solved the Boltzmann equation for the positron momentum distribution taking into account both conduction-electron scattering and acoustic-phonon scattering as means of positron energy loss. According to their calculations, it takes about 3 ps at 300 K, 7 ps at 100 K, and 35 ps at 10 K for the positrons to thermalize to a mean energy of 1.1 times the thermal energy. These are indeed short times compared with the average positron lifetime of 170 ps in Al. The results by Jensen and Walker are in agreement with the experimental ACAR data by Kubica and Stewart.[5]

In all the latest calculations it has been pointed out that phonon scattering is the dominant energy-loss mechanism below 1-eV positron energy.[3,6,7] Practically no attention has,

however, been paid in the literature to the differing cross sections of positron-phonon interaction in different materials. From the classical point of view, it can be expected that in a heavy material, phonon scattering would be less efficient than in a light host. This could perhaps lead to significant differences in the thermalization times between materials. In this paper we have addressed this side of the positron thermalization problem by performing calculations similar to those in Ref. 7 in two different semiconductor materials, Si and GaAs.

Our calculations show that in some materials, positron thermalization down to the 10 K temperature range may take much longer than generally thought. At 10 K in GaAs, for example, it takes about 80 ps for the positrons to reach a mean energy of twice the thermal energy E_{th}, and about 180 ps for the $1.1 \times E_{th}$ level. These times are clearly of the same order of magnitude as the average lifetime in the lattice (230 ps) thereby perhaps leading to observable effects in experimental studies. In Si, the thermalization is much faster: 25 ps for $2 \times E_{th}$ and 70 ps for $1.1 \times E_{th}$.

Besides numerical calculations, the main objective of this paper was to search for evidence of nonthermal positrons experimentally by studying the temperature dependence of the positron trapping rate at negative vacancy-type defects down to very low temperatures. The momentum distribution of thermalized positrons is of the Maxwell-Boltzmann type, and the trapping rate at negative vacancies should increase at least as rapidly as $T^{-0.5}$ (Ref. 8). This is mainly due to the enhancement of the free positron wave-function amplitude at the vacancy site with decreasing positron energy, which in turn increases the transition rate to the vacancy ground state. It is thus the effective positron temperature that is the important concept when considering positron trapping at negative defects. Hence, if thermalization is incomplete or slow, the positron energy does not attain the equilibrium distribution soon enough after the implantation. The effective trapping rate thus cannot increase as rapidly as in the ideal situation and the deviation from the $T^{-0.5}$ behavior can be attributed

to nonthermal positrons. In this experimental approach, the positron energy distribution is monitored when the positrons disappear from the delocalized state either by trapping or annihilation. This is, of course, earlier than the time of annihilation probed in ACAR measurements.

We apply this method to positron trapping at negative divacancies and vacancy-phosphorous complexes in pure Si, and negative Ga vacancies in undoped GaAs. The experimental data in Si is in agreement with the theoretically predicted rather rapid thermalization down to 8 K. In GaAs, the positron lifetime and Doppler-broadening data support the theoretical results of slow thermalization to low temperatures. Our experimental results at various sample temperatures can be even quantitatively explained by the calculated time development of the average positron energy during thermalization. Most importantly, a considerable discrepancy between the measured and calculated data appears if the positrons are assumed to thermalize instantly. All in all, our theoretical and experimental results indicate that the positron thermalization rate may vary from one substance to another more than generally assumed in positron studies.

This paper is organized as follows. The experimental details are explained in the next section (Sec. II). In Sec. III we present the main features of the theory behind the thermalization calculations.[7] This is followed by the numerical results in Si and GaAs (Sec. IV). The experimental data are shown in Sec. V A and the models used to combine the experimental and theoretical results in Sec. V B. The measurement results are discussed in light of the theoretical results in Sec. V C and the final conclusions are presented in Sec. VI.

II. EXPERIMENTAL METHODS

A. Samples

The temperature dependence of positron trapping can be ideally studied in a material containing only one type of a positron trap: a negative vacancy, the concentration of which remains constant at all temperatures. In this paper we have investigated one GaAs and two Si samples.

The GaAs sample was commercial undoped semi-insulating GaAs that contains negative Ga vacancies.[9-11] The Fermi level is pinned at the midgap by the so-called EL2 defects (arsenic antisites) at all temperatures. At this position of the Fermi level, the gallium vacancies are three times negatively charged according to theoretical calculations.[12] This sample is called sample 1.

Both Si samples are floating-zone refined material in which the impurity concentrations are below 1×10^{15} cm^{-3} according to photoluminescence studies. They have both been irradiated with 2-MeV electrons at room temperature. One of the Si samples (2) is pure, highly resistive and has been irradiated to a fluence of 1×10^{18} cm^{-2}. The dominant defect has been identified as the negative divacancy.[13] It is, however, possible that a small fraction of the divacancies are in the neutral charge state in this sample.[13] The other Si sample (3) is of phosphorus-doped ($[P] = 3 \times 10^{16}$ cm^{-3}) n-type material that has been irradiated to a total fluence of 2×10^{16} cm^{-2}. The prevailing

vacancy-type defect in this sample below 90 K temperatures is the negative phosphorus-vacancy pair $(\text{V-P})^-$.[14]

B. Positron spectroscopy

Two independent experimental methods were used to study positron trapping: positron-lifetime and Doppler-broadening measurements.[15,16] The lifetime spectra were recorded with a conventional fast-fast spectrometer with a resolution of 240 ps full width at half maximum (FWHM). The Doppler broadening of the annihilation line was measured with a high-purity Ge detector connected to a digitally stabilized multichannel analyzer. The energy resolution was 1.2 keV (FWHM) at 511 keV. The positron source was 30 μCi of carrier-free ^{22}NaCl enclosed between 2 μm aluminum foils. The source was sandwiched between two identical 5×5 mm^2 samples. Approximately 2×10^6 counts were collected to each lifetime spectrum and 8×10^6 counts to each Doppler spectrum. For the variation of the temperature, the samples were mounted in a closed-cycle He cryostat with a temperature range from 6.5 to 350 K. The temperature was controlled with a resistive 36 W heater and it was measured with a calibrated Au(Fe 0.07%)-Chromel thermocouple attached near the sample. The accuracy of the temperature control was estimated to be better than 0.5 K.

C. Data analysis

The positron lifetime spectra were analyzed in the conventional way.[15-17] After the reduction of a background and annihilations in the source, the spectra were analyzed with one or two exponentials. In the case of two components, the average positron lifetime τ_{av} was calculated as $\tau_{av} = \Sigma I_i \tau_i$ where I_i and τ_i are the intensities and lifetime components from the decomposition, respectively. The average lifetime is a statistically reliable parameter since it is insensitive to the details of the decomposition. Due to the reduced electron density in a vacancy, the characteristic lifetime τ_V is longer than that in the bulk τ_B. Thus, if positrons get trapped at vacancies, the average lifetime increases. In case of only one vacancy type in the sample, the average lifetime can be expressed as $\tau_{av} = (1 - \eta_V)\tau_B + \eta_V \tau_V$. Here, η_V is the fraction of trapped positrons. The value τ_B is obtained by measuring the positron lifetime in defect-free samples and τ_V as the second lifetime in the decomposition of the lifetime spectra.

The Doppler-broadening spectra were characterized with parameters S and W. The S parameter, defined as the fraction of counts in the central part of the 511-keV peak at $|E_\gamma - 511$ keV$| < 0.7$ keV, measures mainly annihilations with low-momentum valence electrons. The W parameter, calculated as the fraction of counts in the wings of the peak at 2.5 keV $< |E_\gamma - 511$ keV $| < 4.2$ keV, is related to the annihilations with high-momentum core electrons. Annihilations in vacancies lead to the narrowing of the annihilation line, i.e., a decrease in W and an increase in S. If a fraction η_V of positrons is trapped at vacancies, the measured S and W parameters can be written as $F = (1 - \eta_V)F_B + \eta_V F_V$ where $F = S$ or W. F_B and F_V are the characteristic Doppler parameters in the defect-free lattice and at the vacancy, respectively. They can be determined by combining positron-lifetime and Doppler-broadening experiments.[15,17]

III. THEORY OF POSITRON THERMALIZATION BY ACOUSTIC-PHONON SCATTERING

The Boltzmann transport equation is well applicable for the positron thermalization problem. Using this approach, Woll and Carbotte[2] calculated the positron thermalization in simple metals considering only conduction-electron scattering as the energy-loss mechanism. A more refined calculation in Al was performed by Jensen and Walker,[7] who also included scattering off longitudinal-acoustic phonons.

The Boltzmann equation determines the time evolution of the positron momentum distribution given an initial distribution and the interactions as input. In a homogeneous medium, the positron momentum distribution $n(\mathbf{q},t)$ at time t is the solution of the following equation:

$$\frac{d}{dt}n(\mathbf{q},t)=\int d^3q'[W(\mathbf{q}',\mathbf{q})n(\mathbf{q}',t)-W(\mathbf{q},\mathbf{q}')n(\mathbf{q},t)]$$
$$-[\lambda+\kappa(\mathbf{q})]n(\mathbf{q},t)+n_{\text{init}}(\mathbf{q},t). \tag{1}$$

Here $n(\mathbf{q},t)d^3q\,dt$ is the probability of finding the positron in a momentum element $\hbar^3 d^3q$ around $\hbar\mathbf{q}$ within time interval $[t,t+dt]$. $W(\mathbf{q},\mathbf{q}')d^3q'$ is the transition rate from momentum $\hbar\mathbf{q}$ to momenta in the volume d^3q' at $\hbar\mathbf{q}'$, which is to be calculated with the Fermi Golden Rule. Further, λ denotes the annihilation rate in the delocalized state, $\kappa(\mathbf{q})$ the momentum dependent trapping rate, and $n_{\text{init}}(\mathbf{q},t)$ represents the initial positron source.

The effect of the trapping and annihilation terms is, of course, to reduce the number of positrons in the distribution. In this paper, we are mainly interested in the shape of the distribution. The annihilation rate λ can be considered momentum independent and the term can be neglected. The trapping rate $\kappa(\mathbf{q})$ at negative vacancies depends on both the concentration of defects and the positron momentum $\hbar\mathbf{q}$. Because of the complexity of its contribution, we concentrate here only on estimating the effect of positron-phonon interactions on thermalization. Hence, also the trapping term is neglected.

Positrons emitted from a radioactive source have a continuous energy spectrum with a mean energy of typically a few hundred keV's. Right upon penetration into the solid sample, the energy-loss rate of positrons is very high: the mean energy decreases to eV level in less than 5 ps by electronic excitations.[6] Below 1-eV energies, the phonon scattering has been shown to dominate over conduction-electron scattering in various metals.[3,6,7] As an example, if only electrons are taken into account when calculating the positron thermalization in Al down to 10 K, it would require a time of about 20 000 ps for the positrons to get within 10% of the thermal energy. Including the phonons reduces the time by more than two orders of magnitude. In practice, the role of positron-electron scattering in metals is small when thermalization to temperatures below 300 K is considered. In semiconductors and insulators, the positron-electron scattering mechanism is even less effective due to the presence of the energy gap. Therefore, studying here only semiconductors, we neglect the electron scattering completely. Instead, we assume that at some time during the thermalization, the pos-

itron energy distribution is very close to a MB distribution with an average energy of about half the band gap, and we start the calculation with such a distribution. Thus, the starting time of our calculations ($t=0$ in this paper) corresponds to the time of 0 ps $\leq t \leq 5$ ps after implantation of positrons in typical experiments.

Positrons scatter off both acoustic and optical phonons in Si and GaAs. The scattering rate off transverse-acoustic phonons is practically zero due to the momentum conservation. During thermalization, the positron energy loss via optical-phonon emission ceases to play a role after the positron energies decrease below the minimum phonon energies, 64 meV in Si and 35 meV in GaAs.[18] These threshold values are so high that also positron scattering via optical-phonon absorption at sample temperatures below 100 K can be neglected.[19,20] Hence, as we concentrate on positron thermalization to very low temperatures, we take only the longitudinal-acoustic phonons into account in this paper. For them we apply the Debye approximation.

The transition rate $W(\mathbf{q}',\mathbf{q})d^3q'$ from volume d^3q' around $\hbar\mathbf{q}'$ to momentum $\hbar\mathbf{q}$ can be estimated by the Fermi Golden Rule.[21] With longitudinal-acoustic phonons, the deformation-potential theory[22] gives us the Hamiltonian $H'=E_{\text{def}}\nabla\cdot\mathbf{u}(\mathbf{R})$, where E_{def} is the positron deformation-potential parameter and $\mathbf{u}(\mathbf{R})$ the lattice displacement of an atom whose equilibrium site is at $\mathbf{R}$. A rather straightforward calculation gives

$$W\left(\sum_{\mathbf{q}'}\mathbf{q}',\mathbf{q}\right)=\frac{2\pi}{\hbar}\sum_{\mathbf{q}'}|\langle\mathbf{q}|H'|\mathbf{q}'\rangle|^2\delta(E_f-E_i)$$
$$\times\delta(\mathbf{q}-\mathbf{q}'\pm\mathbf{k})$$
$$=\int d^3q'\,W_{\text{ph}}(\mathbf{q}',\mathbf{q}), \tag{2}$$

with

$$W_{\text{ph}}(\mathbf{q}',\mathbf{q})=\frac{\gamma^2}{4\pi^2}k\{[f_B(\hbar c_s k)+1]$$
$$\times\delta[E_+(\mathbf{q}')-E_+(\mathbf{q})-\hbar c_s k]\delta_{\mathbf{q}',\mathbf{q}+\mathbf{k}}$$
$$\times\Theta(\omega_D-c_s k)+f_B(\hbar c_s k)$$
$$\times\delta[E_+(\mathbf{q}')-E_+(\mathbf{q})+\hbar c_s k]\delta_{\mathbf{q}',\mathbf{q}-\mathbf{k}}$$
$$\times\Theta(\omega_D-c_s k)\}. \tag{3}$$

Here we use the Debye approximation for the phonon dispersion relation, $\omega=c_s k$, where c_s is the velocity of the acoustic waves in the material and k the length of the phonon wave-vector $\mathbf{k}$. ω_D denotes the Debye cutoff frequency that is calculated from the Debye temperature Θ_D as $\omega_D=k_B\Theta_D/\hbar$. In the deformation-potential approximation, the square of the positron-phonon coupling constant is $\gamma^2=E_{\text{def}}^2/2NMc_s$. N is the ion density and M the ion mass, $f_B(E)$ denotes the Bose-Einstein distribution $\{f_B(E)=[\exp(E/k_BT)-1]^{-1}\}$ and $E_+(\mathbf{q})=\hbar^2q^2/2m^*$ the energy of a positron with an effective mass m^*. Θ is the step function.

Assuming that the positron momentum distribution $n(\mathbf{q},t)$ is isotropic, the distribution of momentum magnitudes $g(q,t)$ can be calculated as

$$g(q,t)dq = 4\pi q^2 n(\mathbf{q},t)dq, \qquad (4)$$

$$g_{\text{init}}(q,t)dq = 4\pi q^2 n_{\text{init}}(\mathbf{q},t)dq. \qquad (5)$$

By taking the time derivative of Eq. (4) and using the reduced form of the Boltzmann equation [Eq. (1)] as discussed above, we obtain the required equation that allows us to solve $g(q,t)$:

$$\frac{d}{dt}g(q,t) = 4\pi q^2 \frac{d}{dt}n(\mathbf{q},t)$$

$$= q^2 \int d\varphi_{\mathbf{q}',\mathbf{q}} \int d\theta_{\mathbf{q}',\mathbf{q}} \sin\theta_{\mathbf{q}',\mathbf{q}}$$

$$\times \int dq' W(\mathbf{q}',\mathbf{q})g(q',t)$$

$$- \int d\varphi_{\mathbf{q}',\mathbf{q}} \int d\theta_{\mathbf{q}',\mathbf{q}} \sin\theta_{\mathbf{q}',\mathbf{q}} \int dq' q'^2$$

$$\times W(\mathbf{q},\mathbf{q}')g(q,t) + g_{\text{init}}(q,t)$$

$$= I_1(q,t) - I_2(q,t) + g_0(q)\delta(t). \qquad (6)$$

Here, the function $g_0(q)$ gives the initial positron momentum distribution. Substituting the interaction rates $W_{\text{ph}}(\mathbf{q}',\mathbf{q})$ in the form of Eq. (3) for $W(\mathbf{q}',\mathbf{q})$ in Eq. (6) and performing the integrations gives the following expressions for $I_1(q,t)$ and $I_2(q,t)$:

$$I_1(q,t) = \frac{\gamma^2 m^*}{2\pi\hbar^2}$$

$$\times \left[q \int_{a_1}^{b_1} dk \frac{g[(q^2+2m^*c_s k/\hbar)^{1/2},t]}{q^2+2m^*c_s k/\hbar} k^2 \right.$$

$$\times \left(1 + \frac{1}{\exp(\hbar c_s k/k_B T)-1}\right)$$

$$+ q \int_{a_2}^{b_2} dk \frac{g[(q^2-2m^*c_s k/\hbar)^{1/2},t]}{q^2-2m^*c_s k/\hbar}$$

$$\left. \times \frac{k^2}{\exp(\hbar c_s k/k_B T)-1} \right], \qquad (7)$$

$$I_2(q,t) = \frac{\gamma^2 m^*}{2\pi\hbar^2} \frac{g(q,t)}{q} \times \left[\int_{a_1}^{b_1} dk \frac{k^2}{\exp(\hbar c_s k/k_B T)-1} \right.$$

$$\left. + \int_{a_2}^{b_2} dk k^2 \left(1 + \frac{1}{\exp(\hbar c_s k/k_B T)-1}\right) \right]. \qquad (8)$$

The integration intervals are obtained by requiring the conservation of energy and momentum, and by restricting the wave-vector k to values below the Debye cutoff wave-vector $k_D = \omega_D/c_s$. The resulting limits are the following:

$$a_1 = \max[0, 2(m^*c_s/\hbar - q)],$$

$$b_1 = \min[\omega_D/c_s, 2(m^*c_s/\hbar + q)],$$

$$a_2 = 0,$$

$$b_2 = \min[\omega_D/c_s, \max\{0, 2(q - m^*c_s/\hbar)\}].$$

IV. NUMERICAL RESULTS

The material-related parameters used in the calculations are presented in Table I. The positron deformation potential is obtained from theoretical calculations.[23] Good estimates for the effective mass can be found from experimental positron diffusion studies[24] that probe the same positron-phonon interactions as we do in this study. For c_s, we use the velocity of longitudinal-acoustic phonons in the [110] direction[25] that represents an estimate of the average velocity over all principal directions.

In the actual numerical calculations, the positron momentum range was discretized into 300 mesh points. This mesh was updated regularly such that it covered only the range in which the distribution $g(q,t)$ is significantly above zero. An IMSL Fortran library routine DIVPRK was used to solve the system of ordinary differential equations, Eq. (6). The routine uses the Runge-Kutta-Verner fifth-order and sixth-order methods.[26] The time steps were chosen densely enough so that only small changes took place between the steps. A relative accuracy in $g(q,t)$ better than 10^{-3} was required in each time step throughout the calculation.

Our program was tested by performing a similar calculation in Al as Jensen and Walker did in Ref. 7. For this calculation we included the conduction-electron scattering in our program. After a careful investigation we believe that there is a mistake in their calculation related to the phonon-scattering part. We get exactly the same results as they did if we deliberately multiply the phonon scattering rates [Eqs. (7)

TABLE I. Material parameters used in the thermalization calculations.

Material	E_{def} (eV)	m^* (m_e)	c_s (m/s)	Θ_D (K)	N $(10^{22}$ cm$^{-3})$	M (proton masses)
Si	-6.19[a]	1.6[b]	9130[c]	645[c]	4.96	28.1
GaAs	-5.87[a]	1.3[b]	5230[c]	344[c]	4.42	72.3

[a]Reference 23.
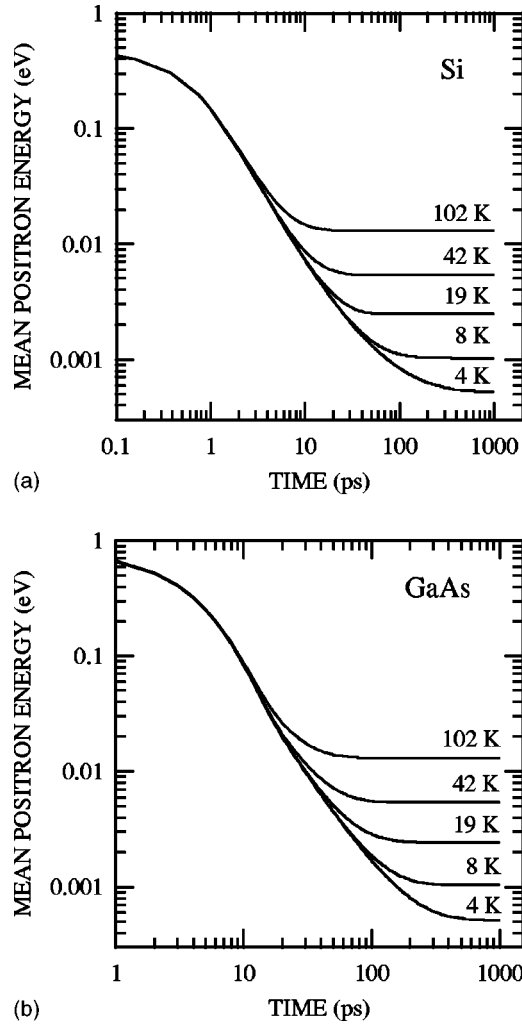[b]Reference 24.
[c]Reference 25.

FIG. 1. The positron mean energy as a function of time during thermalization in (a) Si and (b) GaAs at various sample temperatures. The curves are based on solving the Boltzmann equation for the positron momentum distribution. The calculation was started ($t=0$) at the mean energy of 0.5 eV in Si and at 0.8 eV in GaAs. Only positron scattering with longitudinal-acoustic phonons was included in the calculation.

and (8)] by an extra factor of 2. Thus, the thermalization times given in Ref. 7 are too short by a factor of about 2.

In Figs. 1(a) and 1(b) we present the calculated positron mean energy as a function of time at various temperatures for Si and GaAs, respectively. The mean energy was calculated as

$$\bar{E}(t) = \int dq (\hbar^2 q^2 / 2m^*) g(q,t). \qquad (9)$$

The results show that the mean energy declines along a unique path characteristic of the material irrespective of the sample temperature, except near thermal equilibrium where the curves flatten out. In Si, the variation of the initial mean energy $\bar{E}(t=0)$ from 0.4 to 0.8 eV has in practice no influence on $\bar{E}(t)$ at $t \geq 10$ ps. The same was observed for GaAs at $t \geq 30$ ps with starting energies 0.5–0.9 eV. Thus, the
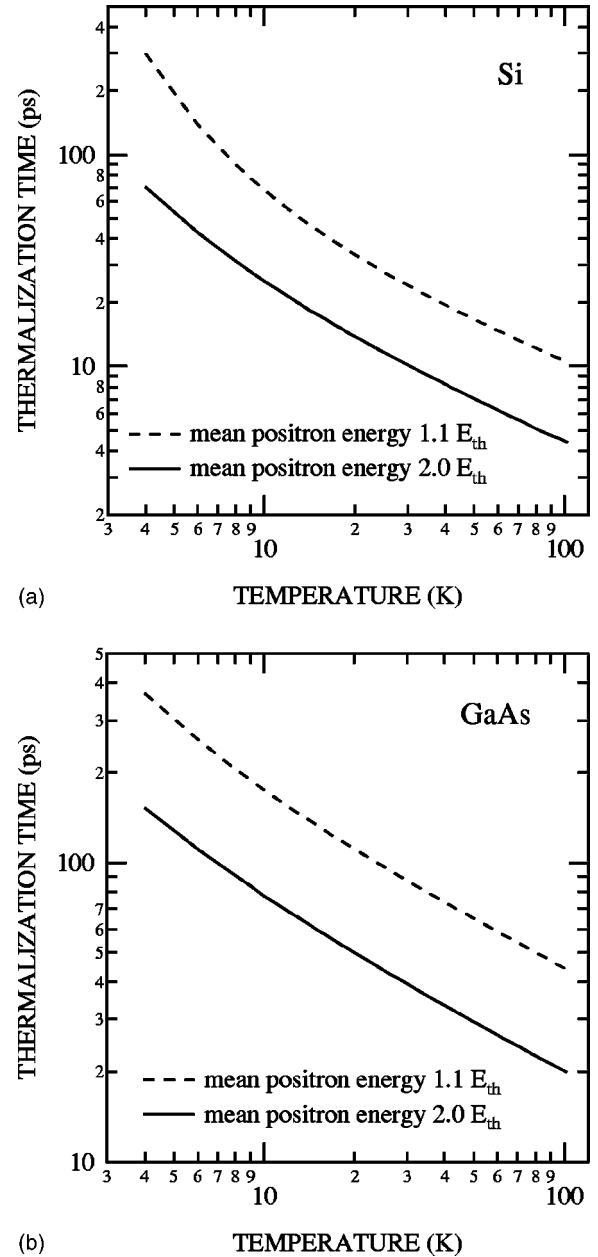

FIG. 2. The positron thermalization time vs sample temperature in (a) Si and (b) GaAs. The solid curves indicate the time needed for the positrons to reach the mean energy equaling twice the thermal energy. The dashed lines again represent the level of 1.1 $\times E_{th}$.

choice of the initial energy is not important when considering temperatures below 100 K.

In Fig. 2 we show how much time is required for the positrons to reach the mean energies of $2 \times E_{th}$ and 1.1 $\times E_{th}$. After reaching the latter energy, the positrons appear as fully thermalized particles from the experimental point of view. In Si [Fig. 2(a)], thermalization even down to 10 K seems to be rather fast: positrons get within 10% of the final thermal energy in 70 ps. Below 10 K, complete thermalization, however, takes a time that is comparable to the mean lifetime in the lattice ($\tau_{Si}=218$ ps). In GaAs [Fig. 2(b)], thermalization times are considerably longer than in Si at all

temperatures. At 10 K it takes about 80 ps for the positrons to reach a mean energy of $2 \times E_{th}$, and about 180 ps for $1.1 \times E_{th}$. At 4 K it takes nearly 400 ps for the thermalization within 10% of the sample temperature. It could be expected that these thermalization times result in experimentally observable effects in GaAs since they are of the same order of magnitude as the positron lifetime in the lattice (τ_{GaAs} =230 ps).

The calculations indicate that depending on the temperature (4–100 K), the thermalization times in GaAs are 2-4 times longer than in Si. This is mainly due to the difference in the mass densities of the materials. Namely, the positron energy-loss rate is inversely proportional to this quantity [see Eq. (3)]. Ga and As are much heavier atoms than Si, and the ratio of the mass densities is 2.5, which thus largely explains the observed difference in the thermalization times.

In addition to the mass density, the energy-loss rate also depends on the positron deformation potential E_{def} and the effective mass m^*. In GaAs and Si, they have relatively similar values (see Table I) leading only to a minor contribution to the difference in the thermalization rate. Further, the scattering rate is inversely proportional to the velocity of the acoustic waves c_s. On the other hand, the average energy released by the positron in the phonon emission is directly proportional to c_s. Thus, the energy-loss rate that is proportional to the product of the scattering rate and the average energy released in the scattering event, is independent of c_s. A numerical calculation by solving Eq. (6) with variable values of c_s confirms that this simple argument seems to be valid relatively accurately, the effect of c_s being quite small. Hence, although the c_s values, and thereby the hardnesses of GaAs and Si, differ significantly, their role is small when considering the thermalization times. The comparison between the thermalization times in different materials cannot, of course, be fully based on evaluation of the positron-phonon coupling constants γ^2 since also the integrals of Eqs. (7) and (8) play a role.

As a conclusion, the strength of the positron coupling to phonons may vary considerably from one material to another. If the coupling is weak, positron thermalization down to 10 K may take even hundreds of picoseconds which is well of the order of positron lifetime. The main reason for the big difference in the thermalization times in Si and GaAs is the difference in the mass densities. When considering other materials, this quantity, together with the positron deformation potential, determine the thermalization time to very low temperatures.

V. EXPERIMENTAL SEARCH FOR NONTHERMAL POSITRONS

The calculations suggest that there is a clear difference in the thermalization times in Si and GaAs when considering temperatures below 100 K. In Si, positrons thermalize close to 10 K in a time that is well shorter than the lifetime in the lattice, whereas in GaAs it takes a time of the order of lifetime. To get experimental support for the theoretical results, we studied the temperature dependence of positron trapping at negative vacancies.

As positive particles, positrons scan the interstitial space of the lattice and feel neutral and negative vacancies as attractive centers at which they can get trapped. Positron trapping rate κ is defined as $\kappa = \mu c$ where c is the concentration of vacancies. The trapping coefficient μ measures the sensitivity of positrons to a particular vacancy defect. In case of neutral vacancies the positron trapping rate is independent of temperature.[8,27]

There is a wealth of experimental evidence that the positron trapping rate at negative defects increases strongly with decreasing sample temperature, at least down to about 30 K.[9,14,27,28] Theoretically, this is well understood.[8] Before trapping, the positron occupies a delocalized Coulomb wave. The amplitude of the Coulomb wave at a negatively charged trap increases strongly towards lower positron energies, i.e. temperatures. This leads to a larger overlap between the initial and final state wave functions, thus increasing the trapping coefficient and thereby, the transition rate of the positron to the localized vacancy ground state.

The model calculations by Puska *et al.* show that the trapping rate increases at least as rapidly as $T^{-0.5}$ for fully thermalized positrons.[8] The predicted divergence at $T \to 0$ K means that positrons become extremely sensitive to negative defects at low temperatures, if fully thermalized. The divergence, however, may not be observed due to incomplete thermalization, since the mean positron energy is higher than the thermal energy corresponding to the crystal temperature. If the effective trapping rate is observed to increase with decreasing host temperature according to $T^{-\alpha}$ with $\alpha < 0.5$, this can be taken as an evidence of incomplete thermalization.

A. Experimental results

The positron lifetime in the delocalized state (bulk) in GaAs was determined from a *p*-type sample with neither neutral nor negative vacancy defects. The lifetime was constant 228 ps from 8 to 150 K consistently with previous measurements.[9] The undoped sample 1 was studied in darkness where negative Ga vacancies act as the only positron traps.[10,15] The lifetime spectra were decomposed with a second lifetime component of 260 ps in agreement with earlier investigations.[9,10] The average lifetime at 300 K is 231 ps, and it increases rapidly down to 25 K, reaching a value of 239 ps. In Fig. 3, the average lifetime is presented with circles from 8 to 50 K. From 50 to 25 K it increases about 2 ps, but from 25 to 8 K, at the most, 1 ps. The Doppler-broadening data show an effect of the same kind: the *W*-parameter values decrease strongly down to 25 K, but below this the temperature dependence becomes much weaker.

In Si, the positron lifetime in bulk was measured to be 217 ps below 100 K and above this, it increases slightly, reaching 218 ps at 300 K. The average lifetime in the pure silicon sample 2 is about 218 ps in temperatures 200–300 K. Below 200 K, it increases strongly attaining a value of 247 ps at 40 K. The data below 100 K are shown in Fig. 4 with open circles. Between 40 and 20 K, the average lifetime decreases about 5 ps and then it increases again towards
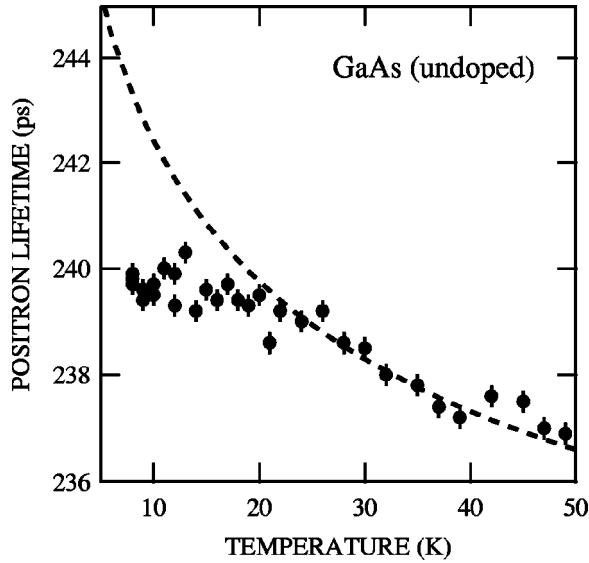
FIG. 3. The average positron lifetime vs sample temperature in undoped GaAs sample 1. The dashed line shows the lowest lifetimes explainable by the theory that assumes the positrons to thermalize instantly after the implantation.

lower temperatures. The second lifetime component in a two-component analysis is 295 ps at temperatures above 40 K. This is the characteristic lifetime of the divacancy.[13] The lifetime τ_2 decreases to 280 ps between 40 and 25 K and remains at that value down to 8 K. The temperature range at which the τ_2 has a lower value than 295 ps coincides with that at which the dip in the average lifetime is seen.

The average lifetime measured in the *P*-doped Si sample (3) increases from 226 ps at 90 K to 233 ps at 30 K. Below 30 K it levels off as can be seen from the data described as closed circles in Fig. 4. The average lifetime from 30 down to 8 K remains more or less unchanged at a value 234 ps. The lifetime data show a constant second lifetime component of 251 ps from 8 to 90 K in agreement with Ref. 14. This is the positron lifetime at negative $(V\text{-}P)^-$ pair.

The experimental positron trapping fraction at Ga vacancies in GaAs can be extracted from the lifetime and Doppler-broadening data by substituting τ or W for F in the formula

$$\eta_V = \frac{F - F_B}{F_V - F_B}. \tag{10}$$

The results are plotted in Fig. 5 from 8 to 120 K. The trapping fraction at Ga vacancies increases from 0.12 at 100 K to 0.35 at 20 K where after, very little increase is observed. Note that Eq. (10) is valid whenever there are only two positron states, the delocalized and the trapped states. It is independent of the details of the thermalization and trapping processes. The conventional relation of the trapping rate, $\kappa = \lambda_B(F - F_B)/(F_V - F)$, is based on the immediate complete thermalization $[t_{\text{therm}} \ll 1/(\kappa + \lambda_B)]$, and cannot be used here.
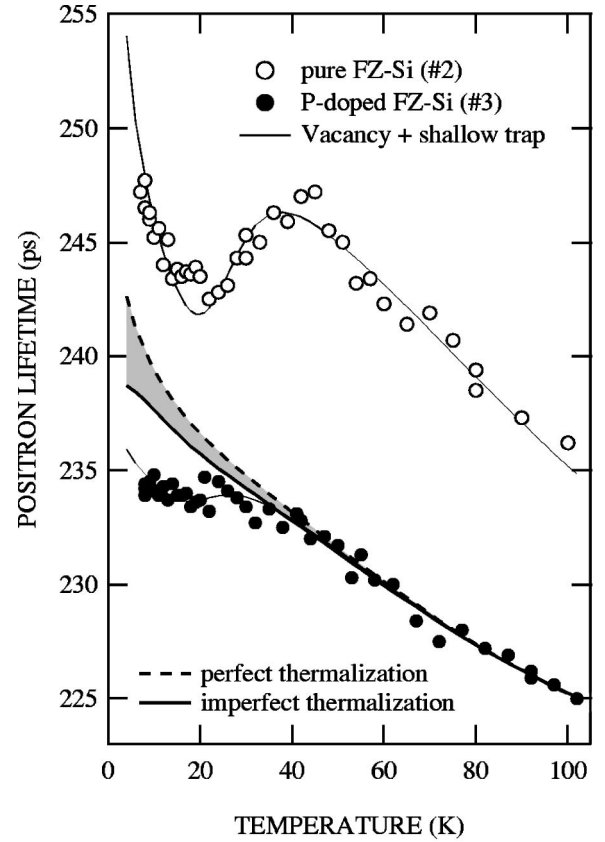

FIG. 4. The average positron lifetime as a function of sample temperature in electron-irradiated FZ-Si. Open circles describe the data measured in the pure sample 2 and the closed circles in the *P*-doped sample 3. The lines describe the best fits with different models that are explained in the text. The shaded area illustrates the effect of incomplete thermalization: the dashed line above the shaded area results from a model assuming instant thermalization and the thick solid line below the shaded area, from a model taking the calculated thermalization effects into account. The thin lines on the data points are based on models that assume fully thermalized positrons getting trapped at vacancies and shallow traps.

B. Modeling of experimental results with thermalization calculations

The effect of incomplete thermalization on positron trapping properties can be evaluated by calculating a time-dependent trapping rate $\kappa(t)$ from the theoretical positron-mean-energy data. The corresponding trapping fraction and the average lifetime can then be derived from $\kappa(t)$. In the following, we will give expressions for these quantities in order to compare the thermalization calculations with the experimental trapping fraction and the average positron lifetime.

Positron trapping at negative vacancy-type defects is dominated by a process in which positrons localize first at shallow Rydberg states acting as precursors for the final transition into the ground state.[8,14] The transition rate from the Rydberg state to the ground state is much faster than the annihilation rate. The positron can also escape from the Rydberg state back to the delocalized states with the aid of thermal energy.[8,29] For fully thermalized positrons, the trap-
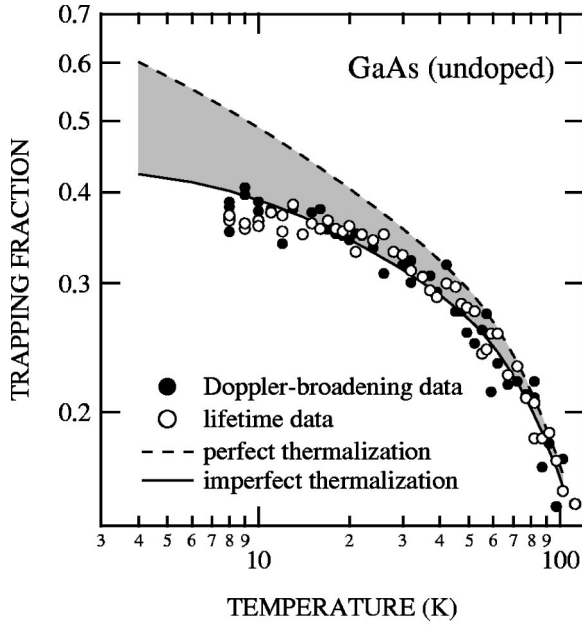
FIG. 5. The positron trapping fraction at Ga vacancies in undoped GaAs sample 1 as a function of sample temperature. The solid line describes the best fit with the model that takes the calculated thermalization behavior into account. If the positrons are assumed to be thermal at the time of implantation, but the same defect-related parameters are used as with the solid-line fit, the temperature dependence of the trapping fraction is that shown by the dashed line. The shading illustrates the effect of imperfect positron thermalization in GaAs.

ping rate at the vacancy ground-state κ and the trapping fraction η_V can be expressed as[15]

$$\kappa = \frac{\dfrac{\mu_0 c_v T^{-0.5}}{N_{at}}}{1 + \dfrac{\mu_0 T^{-0.5}}{N_{at}\eta_R}\left(\dfrac{2\pi m^* m_e k_B}{h^2}\right)^{1.5} T^{1.5}\exp\left(\dfrac{-E_b}{k_B T}\right)},$$ (11)

$$\eta_V = \frac{\kappa}{\lambda_B + \kappa}.$$ (12)

In Eq. (11), both the detrapping and the temperature dependence of the trapping coefficient into the Rydberg state ($\mu = \mu_0 T^{-0.5}$) have been taken into account. c_V denotes the vacancy concentration, N_{at} is the atomic density, η_R the transition rate from the Rydberg state to the vacancy ground state, m^* the positron effective mass, m_e the electron rest mass, k_B the Boltzmann constant, T the absolute temperature, and E_b the positron binding energy at the Rydberg state. At low temperatures where the detrapping is not important ($k_B T \ll E_b$), the trapping rate follows the temperature dependence expected for the trapping coefficient into the Rydberg state ($\kappa \sim T^{-0.5}$). When detrapping plays a role ($k_B T \sim E_b$), the trapping rate at the vacancy decreases with the temperature much more strongly, like $T^{-\alpha}$ where α is typically ~ 1.5.

During thermalization, positrons are not in thermal equilibrium with the crystal, and Eqs. (11) and (12) cannot be applied. A proper way to model the temperature dependence of the trapping fraction would be to implement the transitions between the delocalized states, the Rydberg states, and the vacancy ground states directly into the Boltzmann equation. The modeling of the experimental data would then require a time-consuming iterative procedure of varying the fitting parameters, which we did not attempt. Instead we applied the following simple ideas.

At low sample temperatures, in which detrapping from the Rydberg states is not important, the positron trapping rate at the vacancy ground state is determined by the capture rate into the Rydberg state. This in turn is governed by the overlap between the delocalized and the Rydberg state wave functions, which depends on the delocalized positron-mean-energy $\bar{E}(t)$ as $\bar{E}^{-0.5}$. The time-dependent trapping rate can thus be written as

$$\kappa(t) = \frac{\mu_0 c_V}{N_{at}} T_{positron}^{-0.5} = \frac{\mu_0 c_V \sqrt{1.5 k_B}}{N_{at}} \frac{1}{\sqrt{\bar{E}(t)}},$$ (13)

for which $\bar{E}(t)$ is obtained from Eq. (9).

If detrapping takes place ($k_B T_{sample} \sim E_b$) the overall trapping rate at the vacancy ground state is more difficult to estimate as a function of time. It is clear that during thermalization, the trapping rate $\kappa(t)$ increases with decreasing positron mean energy reaching finally the value given by Eq. (11). We approximate the trapping rate $\kappa(t)$ at higher sample temperatures (detrapping notable) in the following way: In the beginning of thermalization, the positron trapping rate varies according to Eq. (13). When the trapping rate given by Eq. (13) reaches the maximum value calculated from Eq. (11), this value is used for the rest of the time. This approximation is certainly a coarse one, but we stress that no essential conclusions are based on the data in the temperature range in which detrapping is important ($T \gtrsim 60$ K in GaAs).

To calculate the trapping fraction from the time-dependent trapping rate $\kappa(t)$, we first solve the number of positrons in the bulk $n_B(t)$. The relevant kinetic equation and its solution are

$$\frac{dn_B(t)}{dt} = -\lambda_B n_B(t) - \kappa(t) n_B(t),$$ (14)

$$n_B(t) = e^{-\lambda_B t - \int_0^t dt\,\kappa(t)}.$$ (15)

Then, the trapping fraction is found by integration

$$\eta_V = 1 - \int_0^\infty dt\,\lambda_B n_B(t),$$ (16)

and the average lifetime can be calculated simply as $\tau_{av} = (1 - \eta_V)\tau_B + \eta_V \tau_V$. These quantities can be compared with the experimental results of Figs. 3–5.

Notice that in this approach of searching experimental evidence on nonthermal positrons, we probe the positron momentum distribution at the time when the positron disappears

from the delocalized state either by annihilation or trapping [see Eqs. (14)–(16)]. This is earlier than the time of annihilation monitored in ACAR experiments.[4,5] Our method is thus more sensitive to incomplete positron thermalization.

C. Discussion of experimental and theoretical thermalization data

1. GaAs

From previous studies, it is known that the model described above by Eq. (11) is very well compatible with the positron trapping data related to the V_{Ga} from 300 K down to about 30 K.[9,15] When trying to extend the fit to lower temperatures with the present data (Figs. 3 and 5), we find that the best fit follows the data nicely down to 20 K, below which the fit gradually rises above the data. This is seen in Fig. 3 in which the dashed line represents the best fit. Considering the trapping fractions, the difference between the fit (not shown) and the experimental data increases with decreasing temperature being about 30% at 8 K. The parameters of the best fit are the following: $\mu_0 = 60 \times 10^{15}$ s^{-1} $K^{0.5}$, $\eta_R = 300$ ns^{-1} and $E_b = 14$ meV, which are very near to those published in Refs. 11 and 15. Based on this model, the concentration of Ga vacancies is $c_V = 8.4 \times 10^{15}$ cm^{-3}.

The observed experimental trapping fraction increases with decreasing temperature less than predicted by the theory assuming instantly thermalized positrons. This fact is qualitatively in agreement with the idea that imperfect positron thermalization plays a role at low temperatures. The solid line in Fig. 5 describes the best fit by the model that takes the calculated thermalization into account [Eq. (16)]. As can be seen, the agreement is rather good on the whole temperature range. The best fit converges to parameter values $\mu_0 = 60 \times 10^{15}$ s^{-1} $K^{0.5}$, $\eta_R = 130$ ns^{-1}, and $E_b = 16$ meV, which are similar to the values mentioned above. The reduction of the effective trapping coefficient due to incomplete thermalization leads to a slightly higher value for the vacancy concentration, $c_V = 9.8 \times 10^{15}$ cm^{-3}. To clarify the effect of imperfect thermalization on the trapping fraction, we show with the dashed line in Fig. 5 how the trapping fraction would behave if the positrons were thermal at the time of implantation. Here, the model of Eq. (11) has been applied with exactly the same parameters that were used with the solid line fit. The influence of imperfect thermalization is to decrease the trapping fraction such that between 4 and 10 K the decrease is 25–30%.

In Fig. 6 we illustrate the role of imperfect thermalization in GaAs at different levels of trapping fraction. The right axis is numbered to show the average positron lifetime for the case of positron trapping at V_{Ga} with a characteristic lifetime $\tau_{V_{Ga}} = 260$ ps. The curves were generated using a model in which the trapping rate varies as $T^{-0.5}$ with temperature and no detrapping may take place. The dashed lines describe the ideal temperature dependence of the trapping fraction in case the positrons were thermalized immediately after implantation. The effect of the calculated imperfect thermalization is shown with the solid curves under each
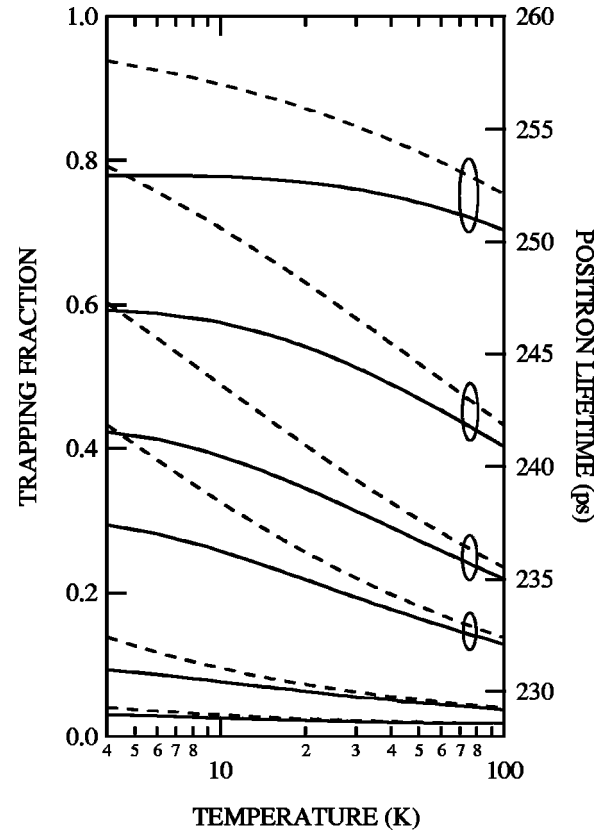

FIG. 6. The effect of imperfect positron thermalization on the positron trapping fraction and the positron average lifetime at various levels of the trapping fraction in GaAs. The dashed lines show the ideal temperature dependence if positrons were in thermal equilibrium with the sample right after the implantation. The solid line under each dashed line was calculated by taking into account the theoretical thermalization data.

dashed one. At 4 K, the relative decrease in the trapping fraction due to the incomplete thermalization is at its largest about 30–35 % at $\eta_V = 0.1 - 0.5$. One also easily finds that the higher the trapping fraction is, the higher the temperature at which the trapping fraction starts to level off. This follows simply from the fact that if the trapping rate is high (e.g., due to high vacancy concentration) fewer positrons remain in the delocalized state and thermalize down to lower temperatures. The leveling off takes place at a sample temperature below which the positrons have no time to cool down to before annihilating or being trapped.

2. Si

The lifetime data measured in the P-doped sample 3 look qualitatively similar to the data measured in sample 1 in GaAs (Figs. 3 and 4). The average positron lifetime in sample 3 is constant between 8–30 K, above which it decreases rapidly. In Fig. 4, the dashed line illustrates the best fit obtained with the model assuming fully thermalized positrons at $t = 0$ [Eq. (11)]. As seen, the model cannot describe the leveling off of the data at the lowest temperatures. The difference between the experimental data and the model val-

ues increases towards low temperatures. Similarly, as in sample 1 in GaAs, this effect is qualitatively explainable with imperfect thermalization.

The solid line bordering the shaded area from below (Fig. 4) shows that taking the imperfect thermalization quantified by our calculations into account improves the fit a little. The curve was calculated using the model described by Eq. (16) with the same parameters that were used with the dashed line fit. Although including the incomplete thermalization extends the explainable region from 40 to 30 K, the model behavior deviates considerably from the experimental data towards the lowest temperatures. The effect of incomplete thermalization at 4 K is about 4 ps. The experimental data clearly cannot be fully explained, even with nonthermal positrons.

In Fig. 4 we also show positron lifetime data in the undoped sample 2. The average lifetime increases rapidly with decreasing temperature down to 40 K, decreases from 40 to 20 K, and then increases again down to the lowest measured temperature of 8 K. Changes in the positron trapping coefficient at negative vacancy-type defects cannot explain this kind of nonmonotonic behavior. This is true irrespective of the positron thermalization properties. Kauppinen *et al.* preliminarily observed this dip in the average positron lifetime in Ref. 13. By comparing the positron-lifetime and Doppler-broadening data in Czochralski- and floating-zone (FZ)-grown samples, they interpreted the temperature dependence with positrons getting trapped at divacancies, and at V-O complexes acting as shallow positron traps. At low temperatures, a fraction of positrons get trapped at V-O complexes in which the characteristic lifetime is much smaller than in the divacancies. This reduces the average lifetime. In Ref. 13 the positron lifetime at the oxygen-related shallow trap was estimated to be 230 ps. Using the positron trapping rate $\kappa_{\text{V-O}} = 0.8(5)$ ns^{-1} calculated similarly as in Ref. 13, and the positron trapping coefficient $\mu \sim 10^{16}$ s^{-1} (Refs. 17,30), we obtain a concentration estimate [V-O]$\sim 10^{15}$ cm^{-3}. This is in agreement with the model in which the rapidly migrating silicon vacancies produced in the electron irradiation couple to residual oxygen atoms forming $\sim 10^{15}$ cm^{-3} V-O pairs.[31]

The data in sample 2 are similar to those of Kauppinen *et al.* and can be explained as follows. Above 40 K, positrons get trapped only at V_2. The increase in τ_{av} is due to both increasing trapping rate at, and decreasing detrapping rate from, the Rydberg states of the divacancies. From 8 to 40 K, positrons also get trapped at the neutral shallow traps. In the range 8–20 K, no detrapping from the shallow traps takes place but the increase in the trapping rate at the divacancies leads to an increase in τ_{av}. Between 20 and 40 K, positrons are able to escape from the shallow traps, which increases the fraction of positrons trapped at the divacancies towards 40 K. This is seen as an increase in the average positron lifetime. This interpretation is supported by the decrease in τ_2 between 20 and 40 K as a result of the combination of two defect lifetimes, $\tau_{V_2} = 295$ ps and $\tau_{\text{V-O}} = 230$ ps. Testing the simple one-defect trapping model with the test quantities $\lambda_{B,\text{test}} = I_1\lambda_1 + I_2\lambda_2$ and $\tau_{1,\text{test}}^{-1} = \tau_B^{-1}[1 + (\tau_{\text{av}} - \tau_B)/(\tau_2 - \tau_{\text{av}})]$ also indicates the presence of more than one defect in

the sample. These observations are identical to those in the work of Kauppinen *et al.* where the effects in τ_{av}, τ_2, and $\tau_{1,\text{test}}$ could be attributed to the V-O complex.[13]

The thin solid curve on the data in sample 2 results from fitting a model with two defects,[15] negative divacancies ($\mu = \mu_0 T^{-0.5}$) and neutral shallow traps (μ_{ST} constant), and assuming that positrons are fully thermalized at $t=0$. As seen, the data is very well described with this model without any consideration on the thermalization. The omission of the imperfect thermalization can be regarded as reasonable since the calculations predict that the effect is rather small in Si above 8 K. Most interestingly, the lifetime data in sample 3 can be explained by introducing a model in which positrons can get trapped at negative (V-P)$^-$ and negative shallow traps ($\mu_{ST} \sim T^{-0.5}$). This is demonstrated by the thin solid line on the data of the *P*-doped sample. This model also explains the Doppler data (not shown). The fitted positron binding energies at the shallow traps in samples 2 and 3 are the same ($E_b = 10$ meV) suggesting that their structures are the same. The assumed difference in the charge states of the shallow traps (neutral in sample 2 and negative in sample 3) follows that of the V-O complex, which is neutral in highly irradiated pure Si and negative in *n*-type Si according to Ref. 32.

In any case, independent of the microscopic structure of the shallow positron traps, the strong increase in the positron lifetime in sample 2 between 8 and 20 K can be regarded as an evidence on rapid positron thermalization in Si in agreement with our calculations. The increase means that the trapping rate at the divacancies has to change considerably in order to induce an increase of 5 ps between 8 and 20 K. Therefore, the mean positron energy also has to decrease efficiently with decreasing sample temperature.

3. Further comments

Lower measurement temperatures are used to improve the sensitivity of positrons to detect negative defects. Our results indicate that the maximum sensitivity in GaAs is attained at around 20 K due to incomplete thermalization whereas in Si, the sensitivity is still improved even below 10 K.

An interesting case for further experimental study of imperfect positron thermalization could be to investigate positron trapping at negative vacancies in germanium. Ge is as heavy as GaAs and, therefore, positron thermalization is expected to take a notable time compared with the lifetime in the lattice. A major advantage considering the experiments is that positron trapping at impurities might be totally avoided since Ge is available with very small impurity concentrations.

VI. SUMMARY

We have studied positron thermalization down to low temperatures in two semiconductors, Si and GaAs, both experimentally and theoretically. The emphasis in our paper was on the possible material related differences in positron thermalization properties.

To find the evolution of the mean positron energy in the material as a function of time upon implantation, we solved

the Boltzmann equation for the positron momentum distribution. The calculations were performed in the temperature range 4–100 K. Only longitudinal-acoustic-phonon scatterings were included as a means of positron energy loss, since other possible excitations have only a minor influence when considering temperatures below 100 K.

As a result of our numerical calculations, we observe that positron thermalization in Si is rather rapid at least down to 10 K: it takes about 25 ps for the positrons to reach the mean energy of twice the thermal energy and 70 ps to get to the level of $1.1 \times E_{th}$. These times are clearly shorter than the positron lifetime in the Si lattice ($\tau_{Si} = 218$ ps). In GaAs, however, thermalization is considerably slower. The time needed by the positrons to reach $2 \times E_{th}$ is 80 ps and $1.1 \times E_{th}$, 180 ps. These times are comparable with the lifetime in the bulk ($\tau_{GaAs} = 230$ ps) thus leading to effects which could be detected experimentally.

The main reason for the different thermalization times in Si and GaAs can be attributed to the differing mass densities: GaAs is much heavier than Si, and the ratio of the densities is 2.5. According to our calculations, the ratio of the thermalization times in GaAs and Si is roughly the same, varying between two and four in the temperature range 4–100 K.

We find experimental support for the calculated thermalization behavior by studying the temperature dependence of the positron trapping rate at negative vacancy-type defects in Si and GaAs. The theory suggests that the trapping rate should increase at least as rapidly as $T^{-0.5}$ with decreasing temperature if the positrons are thermal. Slower variation is expected if a considerable fraction of positrons escape from the delocalized state before thermalization. In the experiments, we found that in GaAs the trapping rate at Ga vacancies below 20 K increases considerably less than expected for fully thermalized positrons. This is an experimental demonstration of incomplete thermalization in GaAs. Taking into account the calculated thermalization results, we can explain the experimental data in GaAs all the way down to 8 K. In Si, the calculations suggest that the effect of imperfect thermalization is of minor importance above 10 K. This result was supported by the experimental data in which the positron annihilation characteristics show strong temperature dependence even down to 8 K.

[1] S. M. Kim, A. T. Stewart, and J. P. Carbotte, Phys. Rev. Lett. **18**, 385 (1967).

[2] E. J. Woll, Jr. and J. P. Carbotte, Phys. Rev. **164**, 985 (1967).

[3] A. Perkins and J. P. Carbotte, Phys. Rev. B **1**, 101 (1970).

[4] P. Kubica and A. T. Stewart, Phys. Rev. Lett. **34**, 852 (1975).

[5] P. Kubica and A. T. Stewart, Can. J. Phys. **61**, 971 (1983).

[6] R. M. Nieminen and J. Oliva, Phys. Rev. B **22**, 2226 (1980).

[7] K. O. Jensen and A. B. Walker, J. Phys.: Condens. Matter **2**, 9757 (1990).

[8] M. J. Puska, C. Corbel, and R. M. Nieminen, Phys. Rev. B **41**, 9980 (1990).

[9] C. LeBerre, C. Corbel, K. Saarinen, S. Kuisma, P. Hautojärvi, and R. Fornari, Phys. Rev. B **52**, 8112 (1995).

[10] K. Saarinen, S. Kuisma, P. Hautojärvi, C. Corbel, and C. LeBerre, Phys. Rev. Lett. **70**, 2794 (1993).

[11] S. Kuisma, K. Saarinen, P. Hautojärvi, C. Corbel, and C. LeBerre, Phys. Rev. B **53**, 9814 (1996).

[12] G. A. Baraff and M. Schlüter, Phys. Rev. Lett. **55**, 1327 (1985); M. Puska, J. Phys.: Condens. Matter **1**, 7347 (1989); H. Xu and U. Lindefelt, Phys. Rev. B **41**, 5979 (1990); S. B. Zhang and J. E. Northrup, Phys. Rev. Lett. **67**, 2339 (1991).

[13] H. Kauppinen, C. Corbel, J. Nissilä, K. Saarinen, and P. Hautojärvi, Phys. Rev. B **57**, 12 911 (1998).

[14] J. Mäkinen, P. Hautojärvi, and C. Corbel, J. Phys.: Condens. Matter **4**, 5137 (1992).

[15] K. Saarinen, P. Hautojärvi, and C. Corbel, in *Identification of Defects in Semiconductors*, edited by M. Stavola (Academic Press, New York, 1998), p. 209.

[16] *Positron Spectroscopy of Solids*, edited by A. Dupasquier and A. P. Mills, Jr. (IOS Press, Amsterdam, 1995); *Positrons in Solids*, edited by P. Hautojärvi, Topics in Current Physics Vol. 12 (Springer-Verlag, Heidelberg, 1979); *Positron Solid State Physics*, edited by W. Brandt and A. Dupasquier (North-Holland, Amsterdam, 1983).

[17] R. Krause-Rehberg and H. S. Leipner, *Positron Annihilation in Semiconductors* (Springer, Heidelberg, 1999).

[18] *Data in Science and Technology: Semiconductors, Group IV Elements and III-V Compounds*, edited by O. Madelung (Springer, Berlin, 1991).

[19] J. Mäkinen, C. Corbel, P. Hautojärvi, and D. Mathiot, Phys. Rev. B **43**, R12 114 (1991).

[20] T. Laine, K. Saarinen, and P. Hautojärvi, Phys. Rev. B **62**, 8058 (2000).

[21] B. K. Ridley, *Quantum Processes in Semiconductors*, 2nd ed. (Oxford University Press, New York, 1988).

[22] J. Bardeen and W. Shockley, Phys. Rev. **80**, 72 (1950).

[23] O. V. Boev, M. J. Puska, and R. M. Nieminen, Phys. Rev. B **36**, 7786 (1987).

[24] E. Soininen, J. Mäkinen, D. Beyer, and P. Hautojärvi, Phys. Rev. B **46**, 13 104 (1992).

[25] Landolt-Börnstein, in *Numerical Data and Functional Relationships in Science and Technology*, edited by O. Madelung, Landolt-Börnstein, New Series, Group III, Vol. 17, Pt. a *Crystal and Solid State Physics* (Springer, Berlin, 1982).

[26] IMSL, Inc., *IMSL MATH/LIBRARY, Fortran Subroutines for Mathematical Applications: User's Manual* (IMSL, Inc., Houston, 1987).

[27] J. Mäkinen, C. Corbel, P. Hautojärvi, P. Moser, and F. Pierre, Phys. Rev. B **39**, 10 162 (1989).

[28] P. Mascher, S. Dannefaer, and D. Kerr, Phys. Rev. B **40**, 11 764 (1989).

[29] M. Manninen and R. M. Nieminen, Appl. Phys. A: Solids Surf. **26**, 93 (1981).

[30] C. LeBerre, C. Corbel, M. R. Brozel, S. Kuisma, K. Saarinen, and P. Hautojärvi, J. Phys.: Condens. Matter **6**, L759 (1994).

[31] G. D. Watkins, in *Deep Centers in Semiconductors*, edited by S.

Pantelides (Gordon and Breach, New York, 1986), p. 147.

[32] J. W. Corbett, *Electron Radiation Damage in Semiconductors and Metals*, Suppl. 7 of *Solid State Physics*, edited by H. Ehrenreich, F. Seitz, and D. Turnbull (Academic, New York, 1966), p. 59.